The Wide Field Monitor onboard the Chinese-European X-ray mission eXTP

Margarita Hernanz[*a,b], Søren Brandt[c], Jean in 't Zand[d], Yuri Evangelista[e,n], Aline Meuris[f], Chris Tenzer[g], Gianluigi Zampa[h], Piotr Orleanski[i], Emrah Kalemci[j], Müberra Sungur[k], Stéphane Schanne[f], Frans Zwart[d], Rob de la Rie[d], Phillip Laubert[d], Coen van Baren[d], Gabby Aitink-Kroes[d], Lucien Kuiper[d], Jörg Bayer[g], Paul Hedderman[g], Samuel Pliego[g], Hao Xiong[g], Riccardo Campana[l], Ettore del Monte[e], Marco Feroci[e,n], Francesco Ceraudo[e], Olivier Gevin[f], Irfan Kuvvetli[c], Denis Tcherniak[c], Konrad Skup[i], Malgorzata Michalska[i], Witold Nowosielski[i], Ander Hormaetxe[a,b], José Luis Gálvez[a,b], Patrícia Ferrés[a,b], Alessandro Patruno[a,b], Walter Bonvicini[m], Matias Antonelli[m], Mirko Boezio[m], Daniela Cirrincione[m], Riccardo Munini[m], Alexandre Rachevski[m], Andrea Vacchi[m], Nicola Zampa[m], Irina Rashevskaya[o], Andrea Argan[p], Onur Turhan[k], Ayhan Bozkurt[j], Ahmet Onat[q], Enrico Bozzo[r], Andrea Santangelo[g], Shuang-Nan Zhang[s], Fangjun Lu[s], Yupeng Xu[s]

[a]Institute of Space Sciences (ICE-CSIC), Carrer de can Magrans, s/n, Campus UAB, 08193 Cerdanyola del Vallès (Barcelona), Spain;
[b]Institut d'Estudis Espacials de Catalunya (IEEC), Barcelona, Spain;
[c]DTU-Space, Technical University of Denmark, Lyngby, Denmark;
[d]SRON Netherlands Institute for Space Research, NL-2333 CA Leiden, the Netherlands;
[e]INAF/IAPS, I-00133 Roma, Italy;
[f]IRFU, CEA, Université Paris-Saclay, 91191 Gif-sur-Yvette, France;
[g]IAAT Universität Tübingen, 72076 Tübingen, Germany;
[h]INFN-Trieste, 34127 Trieste, Italy,
[i]CBK, Space Research Center, Polish Academy of Sciences, PL-00-716 Warszawa, Poland;
[j]Sabanci University, Faculty of Engineering and Natural Sciences, 34956, Istanbul, Turkey;
[k]TÜBITAK-UZAY Space Technologies Research Institute, Ankara, Turkey;
[l]INAF/OAS, Bologna, Italy; [m]INFN Trieste, 34149 Trieste, Italy;
[n]INFN, Sezione Roma Tor Vergata, Via della Ricerca Scientifica, 00133, Rome, Italy;
[o]TIFPA, Trento, 38123 Povo, Italy; [p]INAF, Viale del Parco Mellini 84, I-00136 Rome, Italy;
[q]Electrical and Electronic Engineering, Istanbul Technical University, Ayazağa Campus, Turkey;
[r]DPNC, Geneve University,1205 Geneva, Switzerland;
[s]IHEP -Institute of High Energy Physics, Beijing 100049, China

[*]Contact author: Margarita Hernanz, hernanz@ice.csic.es, www.ice.csic.es

Space Telescopes and Instrumentation 2022: Ultraviolet to Gamma Ray, edited by Jan-Willem A. den Herder, Shouleh Nikzad, Kazuhiro Nakazawa, Proc. of SPIE Vol. 12181, 121811Y · © 2022 SPIE · 0277-786X · doi: 10.1117/12.2628335

ABSTRACT

The eXTP (enhanced X-ray Timing and Polarimetry) mission is a major project of the Chinese Academy of Sciences (CAS), with a large involvement of Europe. The scientific payload of eXTP includes four instruments: the SFA (Spectroscopy Focusing Array) and the PFA (Polarimetry Focusing Array) - led by China - the LAD (Large Area Detector) and the WFM (Wide Field Monitor) - led by Europe (Italy and Spain). They offer a unique simultaneous wide-band X-ray timing and polarimetry sensitivity. The WFM is a wide field X-ray monitor instrument in the 2-50 keV energy range, consisting of an array of six coded mask cameras with a field of view of 180ºx90º at an angular resolution of 5 arcmin and 4 silicon drift detectors in each camera. Its unprecedented combination of large field of view and imaging down to 2 keV will allow eXTP to make important discoveries of the variable and transient X-ray sky and is essential in detecting transient black holes, that are part of the primary science goals of eXTP, so that they can be promptly followed up with other instruments on eXTP and elsewhere.

Keywords: X-ray timing, X-ray spectroscopy, compact objects: black holes, neutron stars and white dwarfs, gamma-ray bursts, X-ray bursts, gravitational wave events, silicon drift detectors, coded mask imaging.

1. INTRODUCTION

The eXTP (enhanced X-ray Timing and Polarimetry) mission[1] has as primary goal the study of matter under extreme conditions of density, gravity and magnetism. But it is also aimed to be a powerful X-ray observatory, acting as a discovery machine of the transient and variable X-ray sky. Its scientific payload includes four instruments: SFA (Spectroscopy Focusing Array), PFA (Polarimetry Focusing Array), LAD (Large Area Detector) and WFM (Wide Field Monitor); see Figure **1** for an artist's impression of the eXTP satellite with all its instruments onboard (see W. Chen et al.[2]). The set of eXTP instruments offers an unprecedented simultaneous wide-band X-ray timing and polarimetry sensitivity. A large European consortium is contributing to the eXTP study, both for the science and the instrumentation. The European consortium is expected to provide two of the four instruments: LAD and WFM; the LAD is led by Italy and the WFM by Spain.

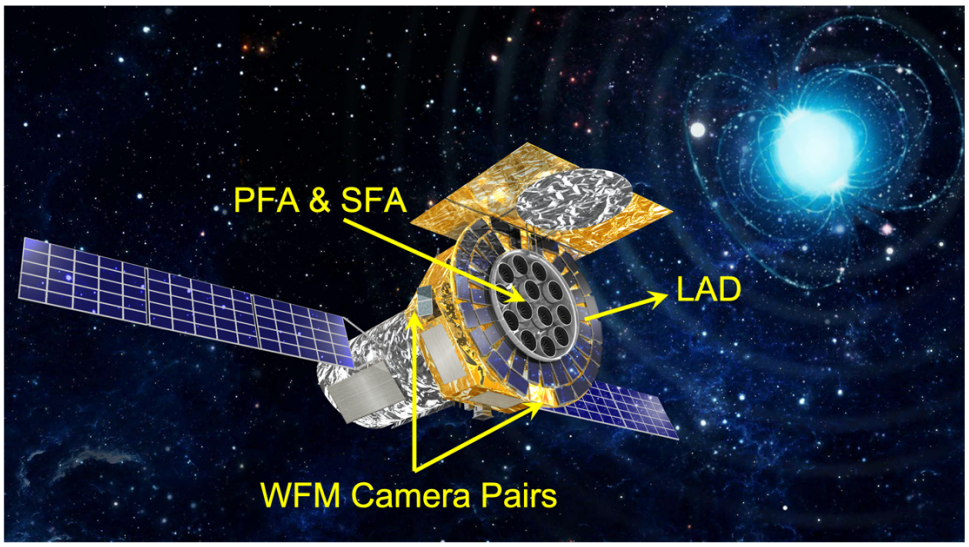

Figure 1. Artist's impression of the eXTP satellite, with its four instruments SFA, PFA, LAD and WFM. Only four of the six WFM cameras are shown; the remaining two are on the opposite side of the spacecraft to the two on the left.

The SFA and PFA instruments are led by China. They include a total of 13 focusing telescopes (9 in the SFA and 4 in the PFA), with 5.25m focal length, effective areas about 0.6 m^2 at (1-2) keV and 300 cm^2 at 3 keV, respectively, and both with timing resolutions of 10 μs and absolute time accuracies of 2 μs (SFA) and 4 μs (PFA). Each one of the 9 SFA focal planes includes an array of SDDs (Silicon Drift Detectors) organized in 19 hexagon cells. These detectors work in the (0.5-10) keV energy range, with an energy resolution better than 180 eV at 6 keV. Each one of the 4 PFA focal planes include a

Gas Pixel Detector, designed in Italy, working in the (2-8) keV energy range, with an energy resolution better than 25% at 6 keV and polarimetric capability.

The LAD instrument includes 40 modules with 4x4 large area Silicon Drift Detectors (SDDs) and 4x4 capillary plate collimators each; therefore, the LAD includes a total of 640 large area SDD detectors. Its effective area at 6 keV is more than 3 m^2 at (8-10) keV, with energy resolution better than 200 eV at 6 keV, time resolution of 10 μs and absolute time accuracy of 2 μs.

See papers from the eXTP session in this conference for more details and updates about the SFA, PFA and LAD instruments.

The development of the WFM is led by Spain. It is based on the design originally proposed for the LOFT ESA M3 mission, that underwent a Phase A feasibility study (the LAD instrument was also part of the LOFT proposal). It is a wide field of view X-ray monitor instrument working in the 2-50 keV energy range. Its focal plane will include large area Silicon Drift Detectors (SDDs), based on the same technology as those used for the LAD but with better spatial resolution, because the WFM will do imaging. The WFM will consist of 3 pairs of coded mask cameras with a total combined field of view (FoV) of 90ºx180º to zero response and a source localization accuracy of ~1 arc min. The main goal of the WFM onboard eXTP is to provide triggers for the target of opportunity observations of the narrow field of view instruments (SFA, PFA and LAD), in order to perform the eXTP core science observation program, dedicated to the study of matter under extreme conditions of density, gravity and magnetism[3,4,5]. In addition, the unprecedented combination of large field of view and imaging capability, down to 2 keV, of the WFM will allow eXTP to make important discoveries of the variable and transient X-ray sky, and provide X-ray coverage of a broad swath of astrophysical objects covered under "observatory science"[6], such as gamma-ray bursts, fast radio bursts and gravitational wave electromagnetic counterparts.

The eXTP mission is expected to be launched by the end of 2027, to an altitude of about 550 km, an orbital inclination below 2.5º, where it will be required to be operational for a duration of 5 years (goal 8 years).

In this paper we provide an overview of the WFM[7] instrument, explaining its design, configuration, and anticipated performance. Details about the current developments for Phase B, as well as the latest news about the WFM will be outlined.

2. SCIENCE OBJECTIVES

2.1 eXTP scientific goals

The eXTP main science drivers correspond to its core science, that deals with three main topics in the astrophysics and fundamental physics domains:

- Dense matter[3]: the goal is to constrain the equation of state (EOS) of ultra-dense matter, like that in the interior of neutron stars. The densities in neutron stars are so large that they are not attainable in terrestrial labs.
- Accretion in strong field gravity[4]: the goal is to test General Relativity in the vicinity of black holes and neutron stars.
- Strong magnetism[5]: the goal is to study the behavior of matter and light in ultra-strong magnetic fields, like in the vicinity of magnetars (highly magnetized neutron stars).

In order to fulfill these goals, eXTP includes three narrow field-of-view instruments (NFIs, specifically the SFA, PFA and LAD), with exceptional spectral-timing and polarization capabilities, and a wide field-of-view instrument (WFM) continuously monitoring the sky for transient sources. In fact, the primary goal of the WFM is to provide alerts about the outbursts of the relevant sources (known or unknown) that should be observed by the NFIs to fulfill the core science objectives: new rare X-ray transients, recurrent X-ray transients, state changes in persistent and transient X-ray sources (black hole and neutron stars mainly). It will have a fast response, providing triggers of active sources in less than about 30s for approximately 65% of the events.

2.2 Observatory science with the WFM

The WFM also has the capability of doing its "own science" - the so-called "Observatory Science" - thanks to its unprecedented combination of wide instantaneous field of view for photon energies down to 2 keV, with excellent imaging and spectral performances. Therefore, in addition and in parallel to providing the crucial triggers to the SFA, LAD and

PFA, the WFM will be monitoring the long-term behavior of hundreds of sources every day, thus allowing us to address not only the eXTP core science topics, but also several other aspects related to the spectroscopic and temporal evolution of both known and new X-ray sources (transients and permanent). It will also detect short (0.1s -100s) bursts and record their data with full resolution.

And last but not least, the WFM will include the XBOT (eXTP Burst Onboard Trigger) capability, a dedicated burst alert system that will enable the distribution to the community of about 100 bursts positions per year, with ~1 arcmin location accuracy within 30 s of the burst trigger, through the Beidou (Chinese navigation and messaging) system. XBOT is based on the heritage of the ECLAIRs instrument onboard the Chinese-French mission SVOM (jointly managed by CAS and CNES) to be launched in the near future. The burst sources will include: GRBs (gamma-ray bursts), FRBs (the recently discovered fast radio bursts), electromagnetic counterparts of GW (gravitational wave) events, and other yet unknown fast events that may be discovered in the future years before eXTP launch. A complete description of the Observatory Science of eXTP, possible thanks to the WFM, can be found in a review paper[6].

2.3 Scientific requirements of the WFM

The main scientific requirements of the WFM are listed in Table **1**.

Table 1: Overview of the main WFM scientific requirements

Item	Requirement / Goal
Point source localization (confidence level 90%)	≤ 1 arcmin / ≤ 0.5 arcmin
Angular resolution	≤ 5 arcmin
Peak sensitivity in the direction of all pointed-instruments (5σ source detection)	1 Crab / 0.8 Crab for an exposure of 1 s, 5 mCrab / 4 mCrab for an exposure of 50 ks
Absolute flux calibration accuracy	20% / 15%
Relative flux calibration precision	5 % / 2.5%
Sensitivity variations knowledge	10% / 5%
Time scales for rate triggers	10 ms - 100 s / 1 ms - 100 s
Rate meter data sampling time	16 ms / 8 ms
Field of view centered at pointing NFIs	≥ π sr = 3.1 sr / 1.75 π sr = 5.5 sr at zero response & 1.33 π sr = 4.2 sr at 20% of peak camera response
Energy range	(2 - 50) keV / (1.5 - 50) keV
Energy resolution	≤500 eV / ≤300 eV
Energy scale calibration accuracy	≤4% / 2%
Number of energy bands for compressed images	≥8 / ≥16
Time resolution	300 s / 150 s for images 10 μs / 5 μs for event data
Absolute time calibration accuracy	2 μs / 1 μs
Event/image data downlink maximum delay	3 hours / 1.5 hours
Onboard storage of triggered date	3 hours
Broadcast of trigger time and position to end user	≤ 30 s / ≤ 20 s after on board detection of the event for 75% of the events
Number of triggers for WFM	≥ 5 per day / ≥ 1 per orbit
Modularity	No loss of full FoV due to single point failure

3. WFM GENERAL DESCRIPTION AND ACCOMMODATION ON THE EXTP SPACECRAFT

The WFM for eXTP is a coded mask instrument[8]. This is a concept already in wide use in past and current instruments for X-ray and gamma-ray astronomy, such as the past instruments GRANAT/SIGMA and BeppoSAX/WFC, and the current ones AGILE/SuperAGILE, INTEGRAL/SPI, IBIS, JEM-X, Neil Gehrels Swift/BAT.

The WFM has a much more compact design than the focusing optics instruments (e.g., SFA and PFA on eXTP), with a very wide FoV, essential for a monitoring instrument. When combined with a convenient detector, it offers the required angular resolution and sensitivity to detect the individual sources for the core science of eXTP. In addition, it can do stand-alone science in a very effective way, thanks to the continuous and simultaneous observation of a large portion of the sky.

The design of the eXTP WFM is based on the concept originally proposed for LOFT (Large Observatory For x-ray Timing), a mission that underwent a phase A study by ESA in the M3 call for "Medium" missions in 2011-2013 (IPRR review in 2013)[9]. The eXTP design consists of six identical (regarding their mechanical, electrical and thermal design) coded mask cameras, arranged in three camera pairs, with each camera covering a FoV of 90° x 90° (full width at zero response), and 30° x 30° (fully illuminated detector plane), respectively.

The central camera pair (cameras 0A and 0B in Figure **2**) points to the viewing direction of the NFIs SFA, LAD and PFA, whereas the other two camera pairs (cameras 1A-1B and 2A-2B in Figure **2**) are tilted +/- 60° relative to that direction. With this specific accommodation of the three WFM camera pairs on the eXTP satellite, the FoV requirement in solid angle of Table **1** is fulfilled (see Figure **3**). The WFM thus succeeds to have an exceptional and unprecedent large FoV, combined with excellent imaging capability in the energy range (2-50) keV, thanks to the coded mask design and the excellent spatial resolution of the SDD detectors.

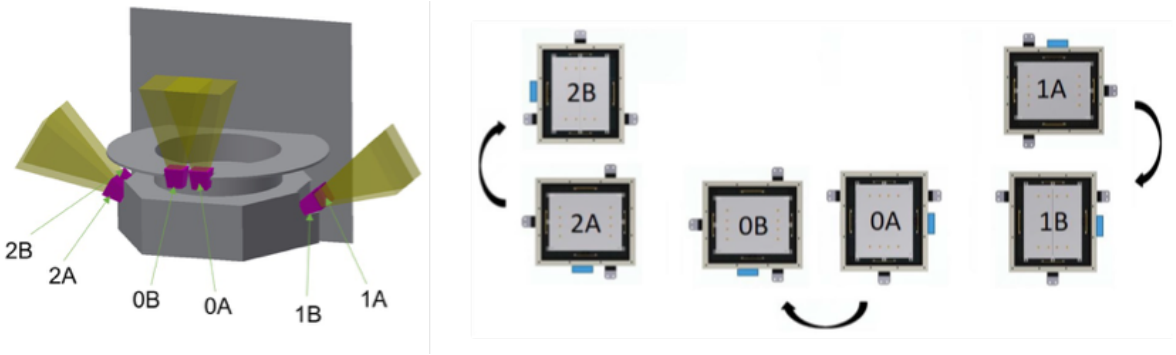

Figure 2: Left panel: the six identical cameras of the WFM, arranged in three camera pairs on the eXTP satellite (see text for details). Right panel: top view of the arrangement of the six WFM cameras.

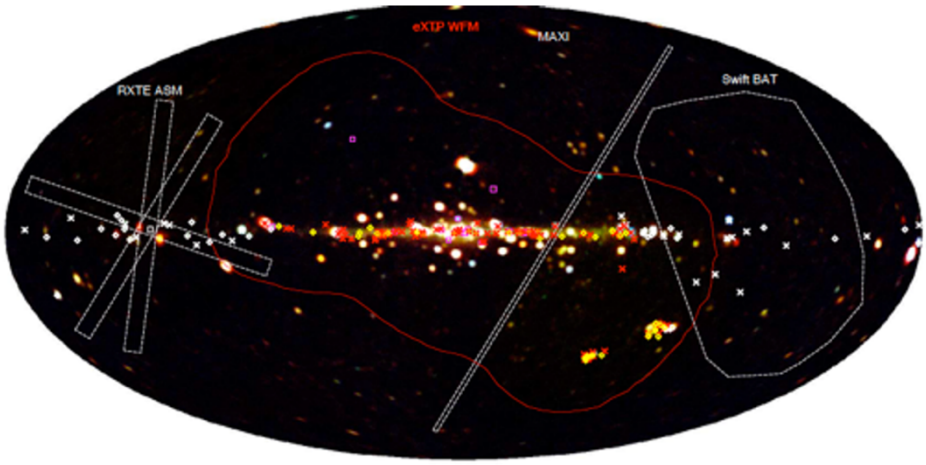

Figure 3: WFM field of view, compared with the most relevant existing facilities (background courtesy of T. Mihara, RIKEN, JAXA and the MAXI team).

4. WFM DESIGN

The WFM includes six identical cameras, grouped in three camera pairs - designated as 0A-0B, 1A-1B and 2A-2B - as shown in Figure **2**. In addition, it has an instrument control unit (ICU), that will be in a separate location on the eXTP satellite.

Each WFM camera includes one detector tray with four detector assemblies (DAs), four Beryllium (or alternative material, like Polypropylene) filters acting as micrometeorite and orbital debris filters for the SDDs, one coded mask assembly with the mask covered by a thermal foil, one collimator, and one back-end electronics assembly (BEE). Each detector assembly (DA) includes a silicon drift detector (SDD), with the corresponding front-end readout electronics (FEE) and mechanical support. The FEE includes, among other components, the ASICs (Application Specific Integrated Circuits), with 24 (12 per SDD side) analogue front-ends. Two additional ASICs, for the Analogue to Digital Conversion (ADC) of the electronic signal, per each DA, are located in the BEE box. The BEE box includes as well the power supply unit (PSU). The ICU includes the power distribution unit (PDU), the data handling unit (DHU) and the buffer memory. The mass memory will be located in the payload data processing unit, which is the computer of the spacecraft dedicated to the payload.

4.1 WFM Functional design

The WFM functional block diagram in Figure **4** illustrates the main functions of the different components of a WFM camera. The main functions of the WFM FEE, BEE and ICU are as follows:

- WFM FEE:
    - forward filtered bias voltages to the SDD sensors
    - provide power and configuration data to the ASICs
    - interface the BEE
    - provide mechanical support to the SDD

- WFM BEE:
    - read-out and analogical/digital (A/D) convert the SDD signals
    - time tagging of the X-ray events
    - trigger filtering
    - pedestal subtraction
    - common mode noise subtraction
    - determination of charge cloud center and width (position in the fine and coarse direction)
    - determination of the total charge collected - correcting for channel gains - to get the energy and perform the event packet generation

- WFM ICU:
    - interfacing the BEEs to the spacecraft computer
    - telecommand (TC) and telemetry (TM) handling
    - instrument monitoring and configuration
    - onboard time management
    - image integration
    - burst triggering, through the eXTP Burst Onboard Trigger system (XBOT)
    - power distribution through the PDU
    - interface with the payload data processing unit of the spacecraft for the mass memory

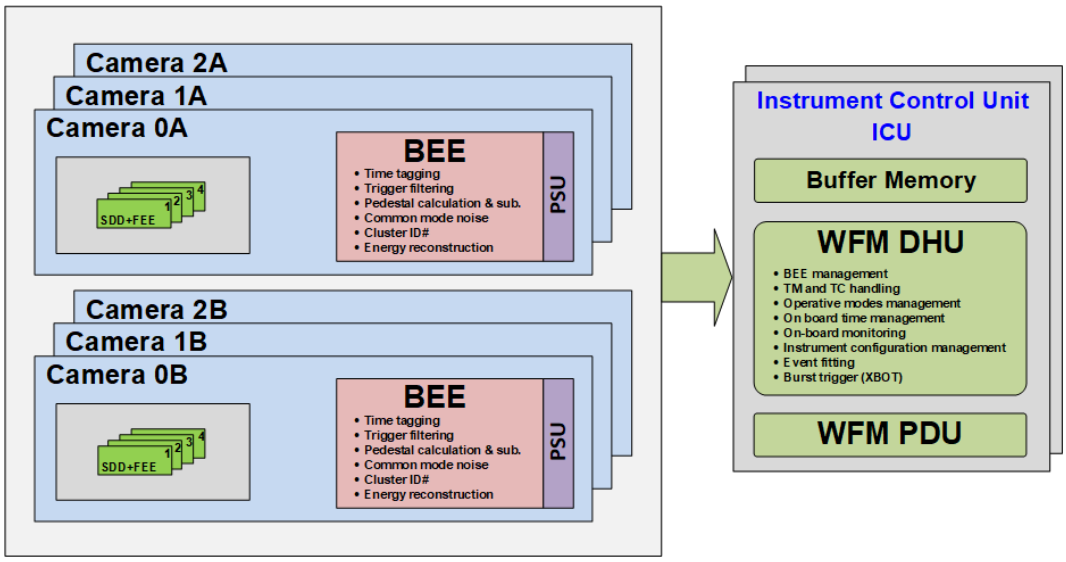

Figure 4: Functional block diagram of the WFM (for details, see text)

4.2 WFM instrument concept and optical design

The design of the WFM cameras is based on the coded aperture imaging concept (see Braga[8]). This technique encodes the sky with a coded mask, which has a pattern of both transparent and opaque zones. Every source within the field of view projects a shadow of the aperture (coded mask with a pattern) on to the position sensitive detection plane; this means that the sky sources illuminate the detector through the coded mask. The deconvolution of the mask shadow in the detector plane permits to recover the position and flux of light sources in the sky, and thus perform imaging.

The particular case of the WFM concept is explained schematically in Figure **5**. Each camera includes four large area SDDs (Silicon drift detectors), similar to those of the eXTP LAD instrument but with better spatial resolution, which is due to a smaller anode pitch (169 μm versus 970 μm). When a photon is absorbed in the SDD, an electron cloud is generated, that drifts towards the anodes. The size of the cloud increases and its size (measured thanks to the small anode pitch that permits to record it on more than one anode) gives rough information of the vertical location of the photon impact, whereas the horizontal location is more accurately provided by the anode position (see Campana et al.[10]). Therefore, SDD detectors provide an asymmetric imaging capability: the photon impinging on the detector will have fine position resolution in the anodes-direction (better than ≈60 μm) and coarse resolution in the drift (perpendicular) direction (better than ≈8 mm), as shown in right panel of Figure **5** (see more details in paper by F. Zwart et al. in these proceedings[11]).

The coded mask pattern has been chosen to well combine with the asymmetric SDD. It consists of 1040x16 open and closed elements, with a mask pitch of 250 μm x 16.4 mm. The open elements (slits) have a minimum dimension of 250 μm x 14 mm, with a spacing of 2.4 mm between the columns (i.e., in the coarse resolution direction). The nominal open mask fraction of the mask is 25% - a value that optimizes sensitivity for weak sources and minimizes telemetry requirements; the effective open mass fraction is in fact 0.85 (14/16.4) times smaller, about 21%.

The angular resolution is obtained from the mask pitch and the mask-detector plane distance (203 mm, see Figure **6**). Therefore, with this combination of detector and mask resolutions, "1.5D" images of on-axis sources with an angular resolution better than 5 arcmin (4.2 arcmin on axis, down to 2.1 arcmin at the FoV edge) in the fine resolution direction times 5° in the coarse resolution direction can be reached, and each WFM camera pair has therefore an angular resolution better than 5 arcmin in both directions.

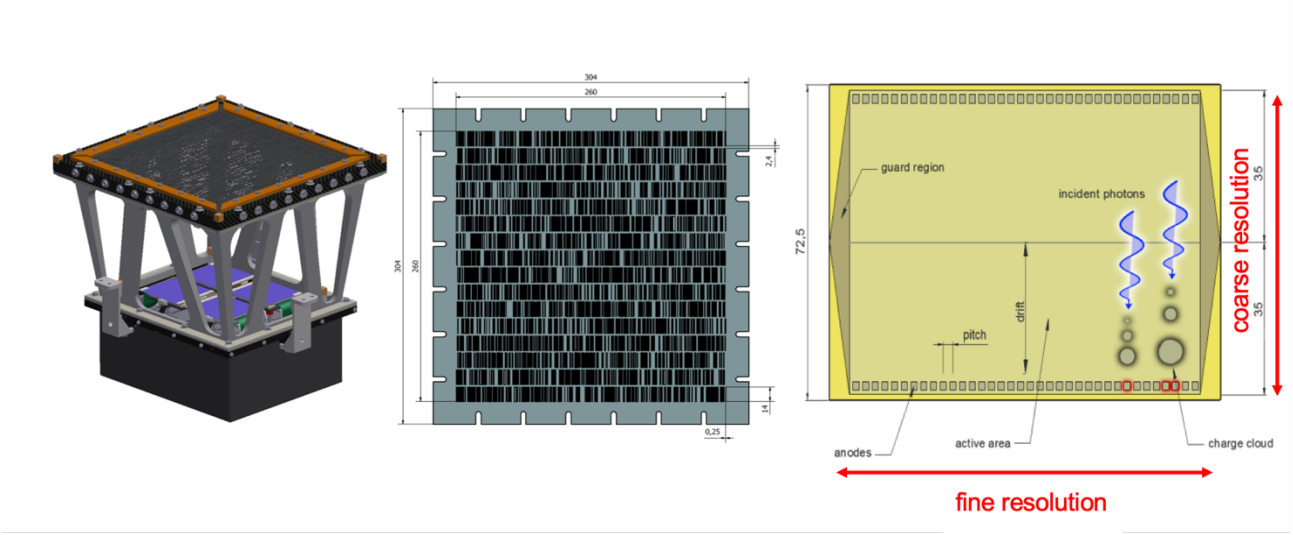

Figure 5. WFM camera concept. Right: scheme of the SDD photon working principle, with indication of the fine and coarse resolution directions (anodes and drift directions, respectively) The anode pitch of the SDDs for the WFM is 169 μm. Middle: coded mask, with the long slit (coarse resolution) and short slit (fine resolution) directions oriented as in the detector. Left: WFM camera with the detector plane - including four detector assemblies in purple - and the coded mask mounted accordingly to the fine and coarse resolution directions. The collimator structure - without its shielding - and the back-end electronic box below are also shown.

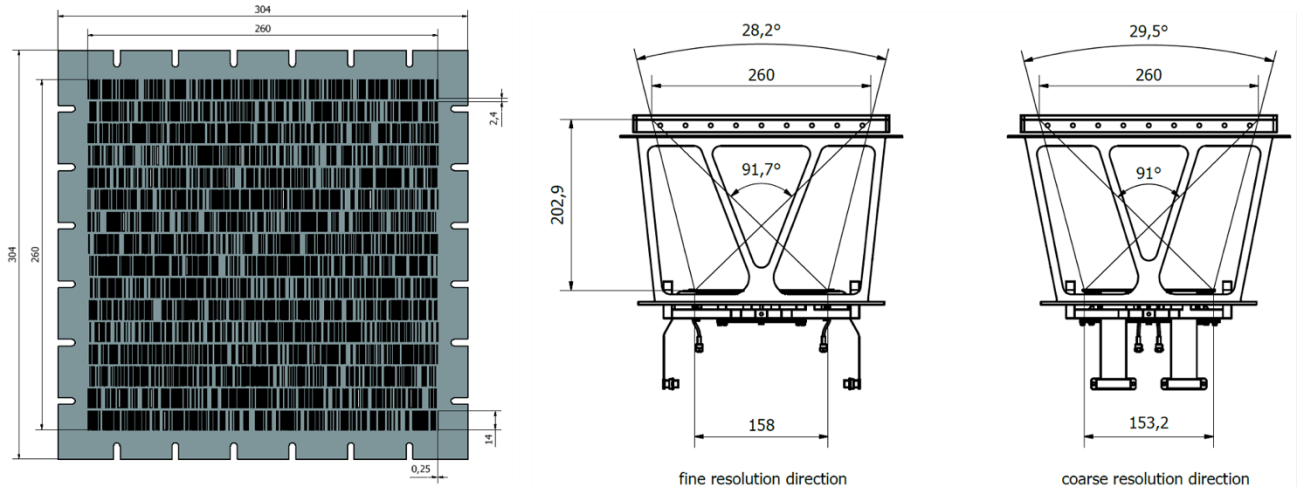

Figure 6: WFM camera optical design. Left: coded mask with dimensions. Right: scheme of the camera with dimensions (both sides)

The way to obtain "2D" imaging with 5 arcmin resolution is to combine two co-aligned cameras orthogonally oriented (see Figure **7**). More details about the optical design of the WFM cameras are shown in Figure **6**. Each camera has a field of view of 90º x 90º (full with at zero response, FWZR) and a fully illuminated FoV of about 30º x 30º.

The design of the WFM is fully modular, with its six cameras arranged in three camera pairs (see Figure **2**). It is important to stress that the cameras could in fact be placed anywhere on the spacecraft (even the two cameras of each one of the camera pairs need not be together). The only condition is that the two cameras in each camera pair are co-aligned and rotated 90º with respect to each other, around their viewing direction (their on-axis direction). The signals of the two cameras in a pair should be combined to give the required 2D images.

The configuration of the WFM is such that the camera pair 0 (cameras 0A-0B in Figure **2**) is pointing on the optical axis of the spacecraft, in the same direction as the LAD, SFA and PFA NFIs of eXTP. The other two camera pairs (1A-1B and 2A-2B in Figure **2**) are tilted away +/- 60º with respect to the on-axis direction. Therefore, the three camera pairs cover a 180º arc, i.e., a field of view of 180ºx90º (full with at zero response, FWZR). This is a large fraction of the sky accessible to the LAD, SFA and PFA. Therefore, the WFM is perfectly suited to provide triggers of the relevant transients (mainly black hole and neutron star binaries entering in outburst phases) for the three NFIs of eXTP.

In addition, the unprecedented simultaneous FoV of the WFM together with its imaging capability and point source localization (1 arcmin) will allow it to do an exciting observatory science (see in 't Zand et al[6]).

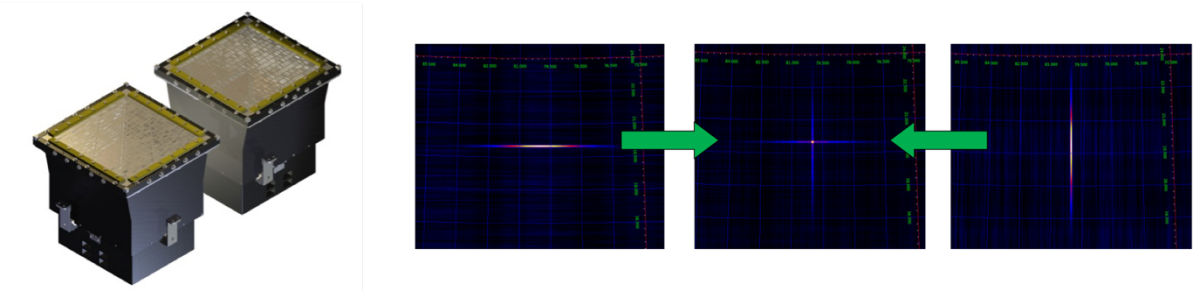

Figure 7: WFM 2D imaging principle. Left: WFM camera pair, where two identical cameras are arranged orthogonally (regarding their coded mask orientations). Right: the combination of the two 1.5D images obtained with each one of the two cameras of a WFM camera pair (right and left figures) gives the 2D image in the central panel. This simulated image corresponds to an isolated source.

4.3 WFM main properties and performance

The main characteristics of the WFM, fulfilling the scientific requirements from Table **1**, are summarized in Table **2**.

Table 2. Main WFM characteristics

Item	**Value**
WFM cameras	6 (arranged in 3 camera pairs)
WFM ICU	2 units (cold redundant)
Mask properties - Optical design	
Mask pattern pitch (pixel size) Size of mask open (slits) and closed elements Mask size	250 μm x 16.4 mm 250 μm x 14 mm 260 mm x 260 mm^2 x 150 μm (thickness)
Mask-detector distance	202.9 mm
Open mask fraction (effective value)	21% (mask pattern 25%)
Detector properties - Optical design	
Detector type - number of SDD tiles	SDD (24 detectors, 4 per camera)
Detector spatial resolution (FWHM)	< 60 μm (fine direction); < 8mm (coarse direction)
Detector operating temperature	- 40 ºC < T < - 21 ºC
Detector size (single)	77.4 mm x 72.5 mm x 450 μm

Item	Value		
Detector active area (single)	64.9 mm x 70.0 mm = 4543 mm^2 = 45.43 cm^2		
	Camera	**Camera pair**	
WFM detectors effective area	182 cm^2	364 cm^2	
WFM peak effective area (on axis, through mask)	> 38 cm^2	> 76 cm^2	
Detector performance			
Energy range	2 - 50 keV		
Energy resolution (FWHM)	< 300 eV at 6 keV		
Optical performance			
	Camera	**Camera pair**	**WFM**
Angular resolution	< 5 arcmin x 5º	< 5 arcmin x < 5 arcmin	< 5 arcmin
Field of view: full width at zero response (FWZR)	90º x 90º	90º x 90º	180º x 90º
Field of view: fully illuminated detectors	30º x 30º	30º x 30º	90º x 30º
Budgets: mass, power, telemetry			
Mass (with margins)	15.6 kg per camera 118.3 kg (total, including ICU)		
Power (with margins)	109.5 W (total, including ICU)		
Average data rate	315 kbits/s		

4.4 WFM mechanical and electrical design

In this section we show a few figures about the mechanical and electrical design of the WFM. We refer the reader to the following detailed complementary SPIE 2022 papers for the details about all the WFM subsystems:

- J-L. Gálvez et al.[14], "The mechanical design and implementation of the WFM cameras for eXTP"
- F. Zwart et al.[11], "The detector/readout-electronics assembly of the eXTP Wide Field Monitor"
- H. Xiong et al.[12], "The digital data processing concepts of the Large Area Detector and the Wide Field Monitor onboard eXTP"
- E. Kalemci et al.[13], "The Instrument Control Unit processing hardware and the software of the Wide Field Monitor on eXTP".

In Figure **8**, the WFM camera layout and its exploded view are displayed.

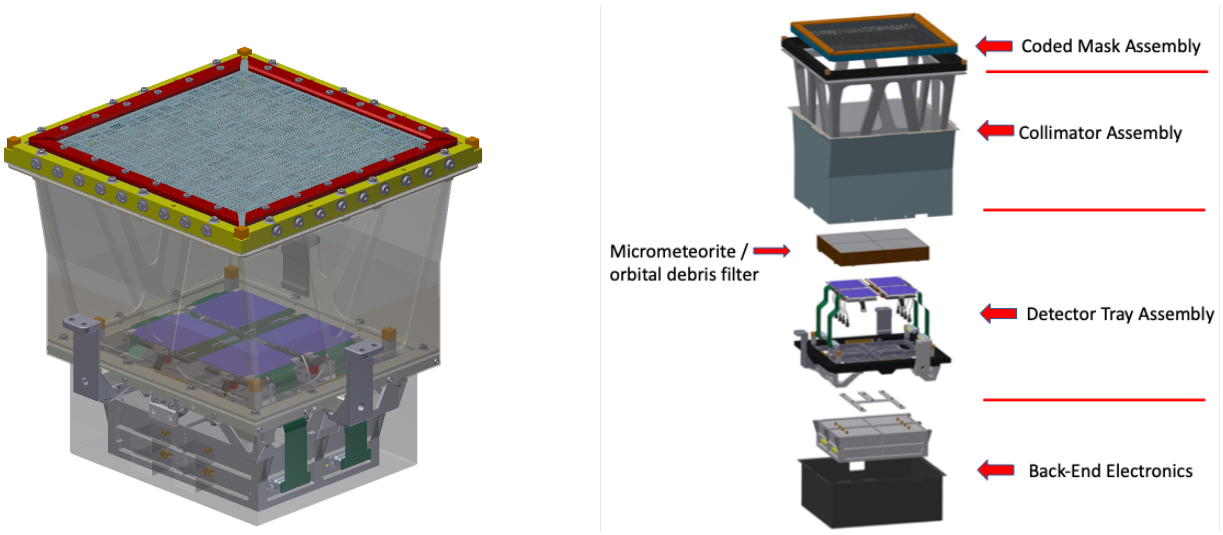

Figure 8: WFM camera mechanical design. Left panel: WFM camera layout, where the coded mask assembly, the collimator and its shielding (transparent), the detector plane with its four detector assemblies and the BEE box are shown. Right panel: Schematic exploded view of a WFM camera.

The WFM detector plane geometry and the assembly including the Beryllium (or Polypropylene) filters protecting the detectors from micrometeorites and orbital debris are shown in Figure **9**.

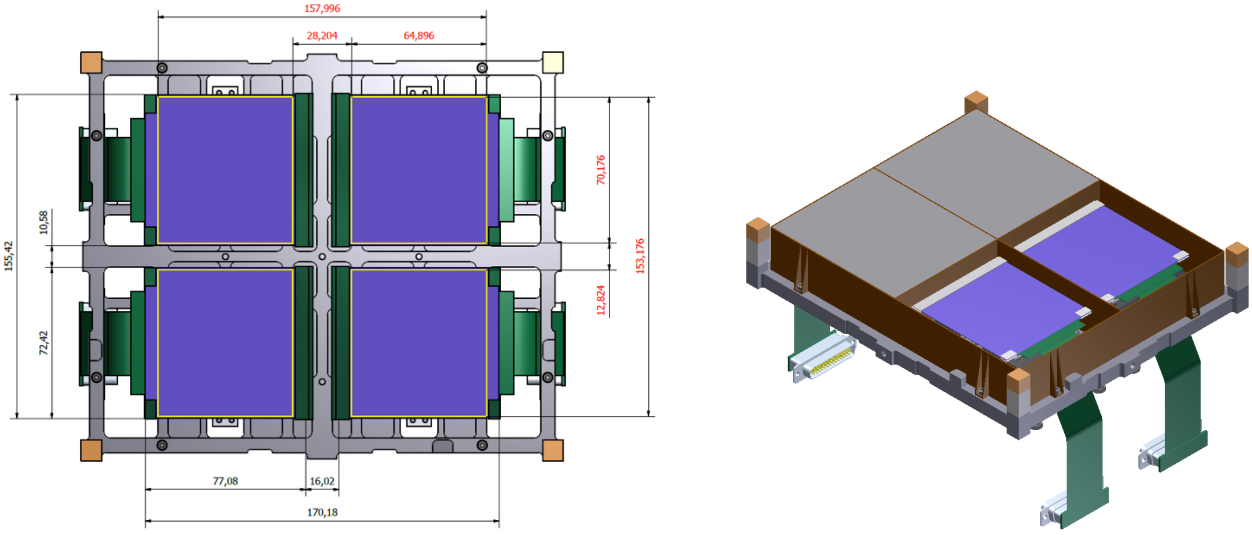

Figure 9. Left panel: top view of the WFM detector plane, including its four detector assemblies and the detector support plate. Right panel: detector plane covered with the four filters (made of Be or Polypropylene) to protect the four SDD tiles from micrometerite (and orbital debris) impacts.

In Figure **10**, one of the four DAs per WFM camera is shown (for more details, see F. Zwart et al. paper about the WFM detector and its readout electronics assembly[11])

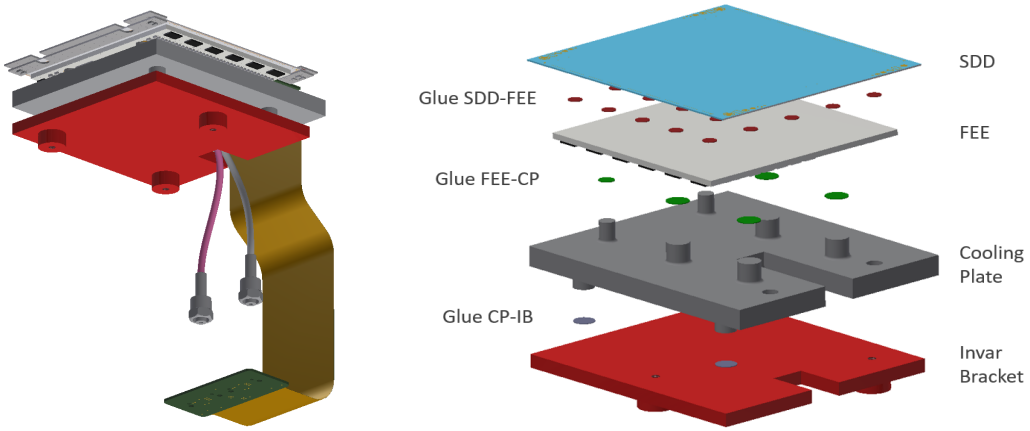

Figure 10. WFM detector assembly (DA). Left panel: layout of the detector assembly, with, from top to bottom, the FEE PCB (Printed Circuit board) including the ASICs and all the FEE components), the cooling plate (gray) and the Invar Bracket (red). The HV (high voltage) and MV (medium voltage) cables are also shown, as well as the flex-print to the BEE. Right panel: scheme of the four layers of the DA, with indication of the glue spots to assembly the corresponding layers one with each other.

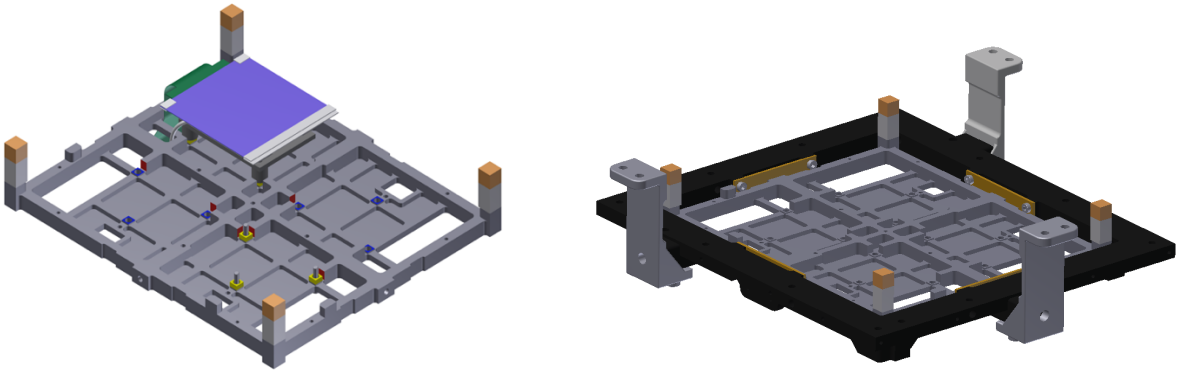

Figure 11: Left panel: WFM detector support plate with one of the four detector assemblies attached.The optical cubes for the alignment with the coded mask are also shown. Right: WFM detector tray support structure, with the detector support plate and the three mounting legs to interface with the camera pair support structure provided by the spacecraft.

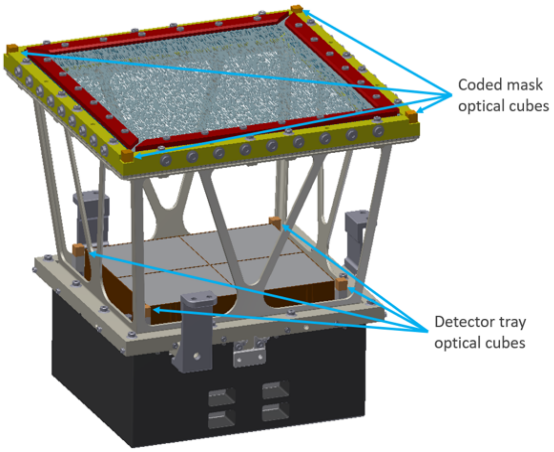

Figure 12: WFM camera with the optical cubes required for the alignment of the detector plane (four detector assemblies) and the coded mask.

In Figure **13**, a detailed scheme of the internal and external electrical and data interfaces of the WFM (cameras and ICU) and the spacecraft is shown. For a more detailed description of the WFM FEE (including SDDs and ASICs), BEE and ICU, see the corresponding papers in these proceedings: F. Zwart et al[11]., H. Xiong et al.[12], E. Kalemci et al.[13].

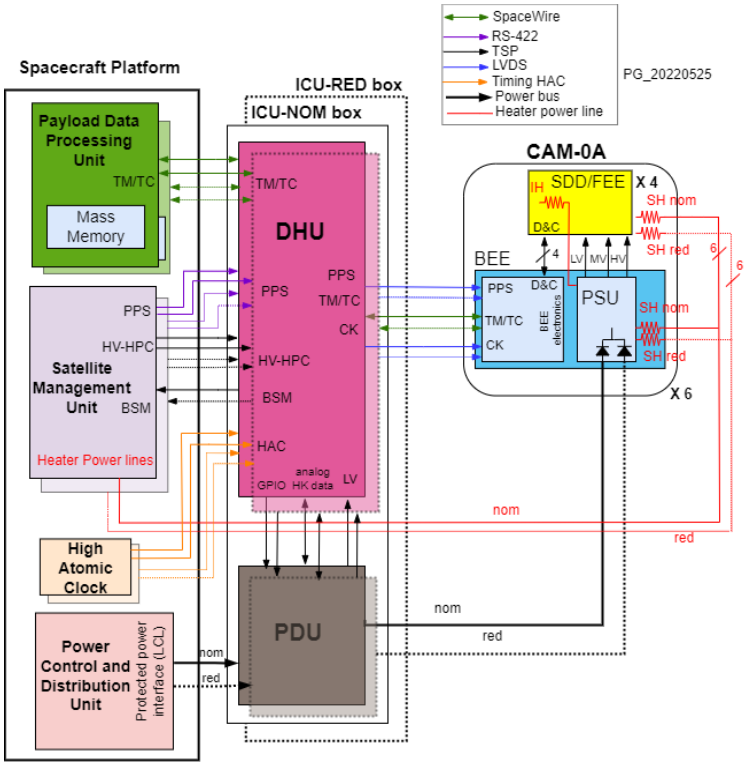

Figure 13: WFM electrical architecture showing all the corresponding interfaces (internal and external)

5. SUMMARY

The WFM of eXTP is a fully modular instrument, offering a simultaneous coverage of a large portion of the sky, thanks to its wide FoV. This makes it essential to trigger the observations of the core science programme sources (mainly black hole and neutron star binaries in outburst) with the narrow-field eXTP instruments. Its unprecedented combination of wide FoV, imaging capability and spectral resolution will provide additional excellent stand-alone science, related to many diverse persistent and transient X-ray sources. It will also discover and study several new short transients, including gamma-ray bursts, fats radio bursts and electromagnetic counterparts of GW events, with fast alert to ground of their position for further observations with other facilities.

ACKNOWLEDGEMENTS

The Spanish authors acknowledge funding support from the MICIN/AEI grant PID2019-108709GB-I00. The Italian authors acknowledge funding support by the Italian Space Agency (under agreement n. 2020-3-HH.0 and ASI-INAF n.2017-14-H.O) and INFN (project XRO - X-ray Observatories).

REFERENCES

[1] Zhang, S.-N. et al., "The enhanced X-ray Timing and Polarimetry mission - eXTP," SCIENCE CHINA Physics, Mechanics & Astronomy (SCPMA) 62, 029502 (2019). http://engine.scichina.com/doi/10.1007/s11433-018-9309-2

[2] Chen, W., Zhu, Z, Xu, Y., Han, X., Chen, Y., Bi, X., Shi, Q., Liu, R., Chao, X., Zhu, C., Zhao, W., Zhang, S.-N., Lu, F., Feroci, M., Hernanz, M., Yuan, H., Yang, Y., He, J., Fang, Y., Zhang; Y., Shi, X., Zhang, K., Yu, J., "Mission analysis and preliminary spacecraft design of the enhanced x-ray timing and polarimetry observatory", Proceedings of the SPIE, vol. 11444, 114442E (2020), https://doi.org/10.1117/12.2562138

[3] Watts, A.L., Yu, W.F. et al., "Dense matter with eXTP", SCIENCE CHINA Physics, Mechanics & Astronomy (SCPMA) 62, 029503 (2019). http://engine.scichina.com/doi/10.1007/s11433-017-9188-4

[4] De Rosa, A., Uttley, P. et al., "Accretion in strong field gravity with eXTP", SCIENCE CHINA Physics, Mechanics & Astronomy (SCPMA) 62, 029504 (2019). http://engine.scichina.com/doi/10.1007/s11433-018-9297-0

[5] Santangelo, A., Zane, S. et al., "Physics and astrophysics of strong magnetic field systems with eXTP", SCIENCE CHINA Physics, Mechanics & Astronomy (SCPMA) 62, 029505 (2019). https://www.sciengine.com/SCPMA/doi/10.1007/s11433-018-9234-3

[6] in 't Zand, J., Bozzo, E. et. al., "Observatory science with eXTP," SCIENCE CHINA Physics, Mechanics & Astronomy (SCPMA) 62, 29506 (2019). http://engine.scichina.com/doi/10.1007/s11433-017-9186-1

[7] Hernanz M., Brandt, S. et al., "The Wide Field Monitor onboard the eXTP mission," Proceedings of the SPIE, vol. 10699, id.1069948, 16pp (2018). https://doi.org/10.1117/12.2313214

[8] Braga, J., "Coded aperture imaging in high-energy astrophysics", PASP, 132, no 1007, p. 012001 (2020).

[9] Brandt, S., Hernanz, M. et al., " The design of the wide field monitor for LOFT", Proceedings of the SPIE, vol. 9144, id. 91442V 20 pp. (2014). https://doi.org/10.1117/12.2055885

[10] Campana, R., Zampa, G., Feroci, M., Vacchi, A., Bonvicini, V., Del Monte, E., Evangelista, Y., Fuschino, F., Labanti, C., Marisaldi, M., Muleri, F., Pacciani, L., Rapisarda, M., Rashevsky, A., Rubini, A., Soffitta, P. Zampa, N., Baldazzi, G., Costa, E., Donnarumma, I., Grassi, M., Lazzarotto, F., Malcovati, P. , Mastropietro, M., Morelli, E., Picolli, L., " Imaging performance of a large-area Silicon Drift Detector for X-ray astronomy", NIMPA, 633, 22-30 (2011). https://doi.org/10.1016/j.nima.2010.12.237

[11] Zwart, F., Tacken, R., in 't Zand, J.J.M., de la Rie, R., Limpens, M., Kochanowski, C., Aitink-Kroes, G., van Baren, C., Bayer, J., Baudin, D., Evangelista, Y., Feroci, M., Frericks, M., Gálvez, J-L., Gevin, O., Hernanz, M., Hormaetxe, A., Laubert, P., Meuris, A., Nab, J., Neelis, J., Tenzer, C., Vogel, C., Zampa, G., "The detector/readout-electronics assembly of the eXTP Wide Field Monitor", these proceedings (2022).

[12] Xiong, H., Argan, A., Baudin, D., Bayer, J., Bouyjou, F., Del Monte, E., Evangelista, Y., Feroci, M., Gálvez, J-L., Hedderman, P., Hernanz, M., Meuris, A., Pliego-Caballero, S., Santangelo, A., Tenzer, C., Trois, A., Wang, X., Zampa, G., "The digital data processing concepts of the Large Area Detector and the Wide Field Monitor onboard eXTP", these proceedings (2022)

[13] Kalemci, E., Turhanb, O., Kuvvetli, I., Schanne, S., Hernanz, M., Orleanski, P., Tenzer, C., Süngur, M., Onath, A., Bozkurt, A., Akif Baltacı, M., Gálvez, J-L., Brandt, S., Skup, K., Tcherniak, D., Michalska, M., "The Instrument Control Unit processing hardware and the software of the Wide Field Monitor on eXTP", these proceedings (2022).

[14] Gálvez, J-L., Hormaetxe, A., Hernanz, M., Ferrés, P., Taubmann, G., Casalta, J. M., Tomás, A., "The mechanical design and implementation of the WFM cameras for eXTP", these proceedings (2022).